Supplementary information for

Transverse electric field dragging of DNA in a nanochannel

Makusu Tsutsui, Yuhui He, Masayuki Furuhashi, Rahong Sakon, Masateru Taniguchi & Tomoji Kawai

The Supplementary Information includes:

1. Supplementary Figures (Fig. S1-S10)

2. Supplementary References

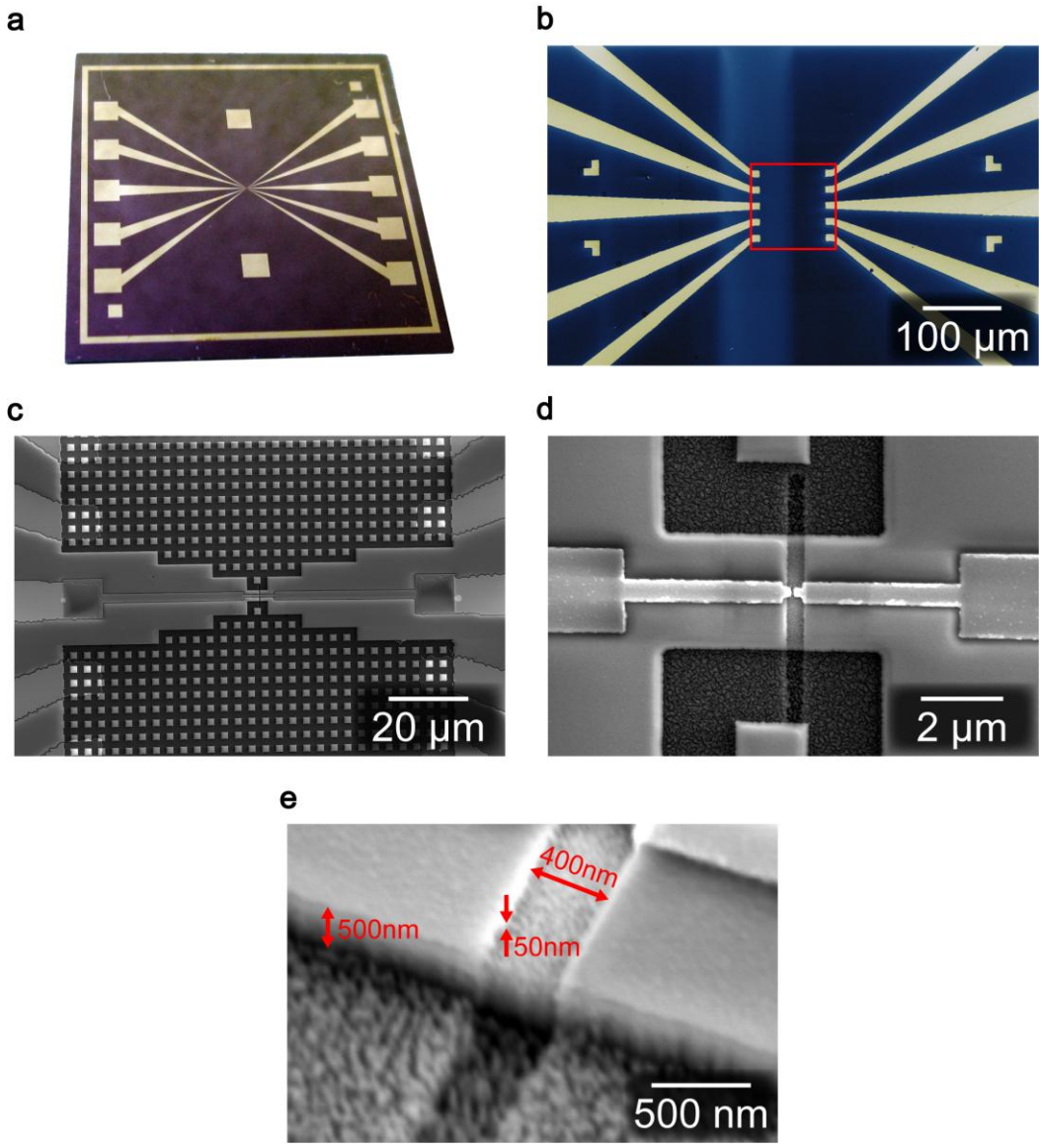

Supplementary Figure S1. Structure of the electrode-embedded nanochannel sensor. **a,** A photo image of the sample chip. Pt/Au/Pt Microelectrodes were formed on a 30 mm square piece of Si/SiO_2 substrate using a photolithography method, magnetron sputtering, and lift-off processes. **b,** A magnified view of the microelectrodes. The L-shaped patterns at both sides of the image were markers used for forming nanochannels in the 100 μm × 100 μm region at the center indicated by the red square. **c-e,** Scanning

electron micrographs showing the structure of a two-leveled electrode channel sensor device. (c-d) It consists of an electrode/nanochannel sensor region and micro-pillar arrays at the upstream and downstream. The electrode gap at the center determines the channel size, which is 200 nm × 50 nm × 60 nm (length × width × height). (e) The sensor region is connected to deeply etched channels of 500 nm height.

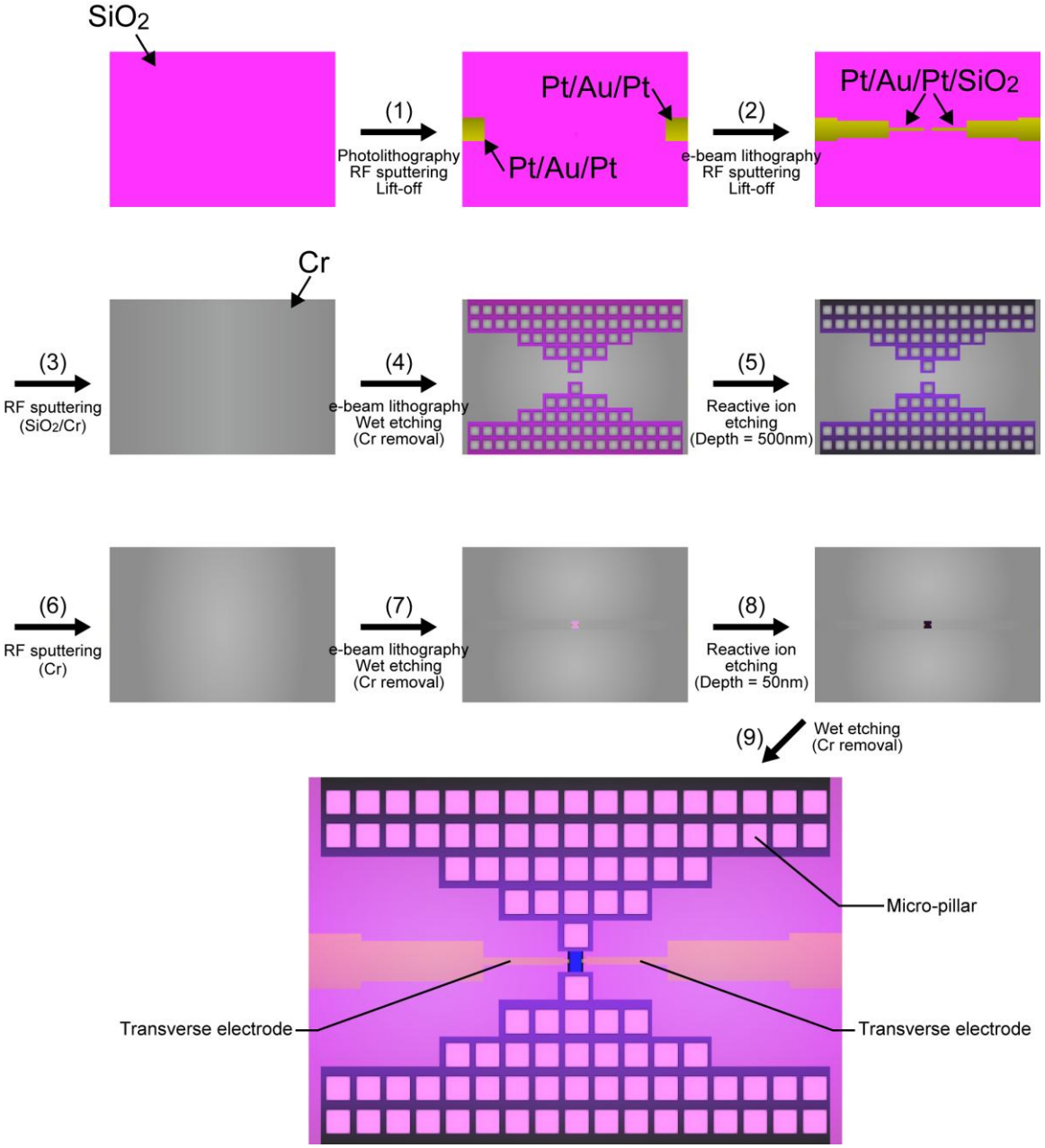

Supplementary Figure S2. Fabrication flow chart of electrode-embedded nanochannel. (1) First, micrometer-scale Au leads (2 nm thick Pt layers were used as an adhesion layer) were formed on a SiO_2-coated Si substrate using a photolithography method, radio-frequency (RF) magnetron sputtering metal deposition, and lift-off processes. (2) After that, a pair of nanoeletrodes with Pt (2 nm)/ Au (30 mn)/ Pt (2 nm)/ SiO_2 (30 nm)

multi-layer structure was fabricated by an electron beam lithography method, RF sputtering, and lift-off processes. (3) The substrate was then coated with SiO_2 (15 nm)/ Cr (100 nm) film. (4) Subsequently, array of squares was lithographically defined and the exposed Cr was removed by a wet etching process. (5) Utilizing the Cr mask, we performed reactive ion etching and fabricated micro-pillars of 500 nm height. (6) We again formed a Cr mask for forming a nanochannel by depositing a 25 nm thick Cr layer and (7) patterning a channel by an electron beam lithography followed by Cr removal using a wet-etching process. (8) Finally, the sample is exposed to the dry etching and (9) residual Cr was removed.

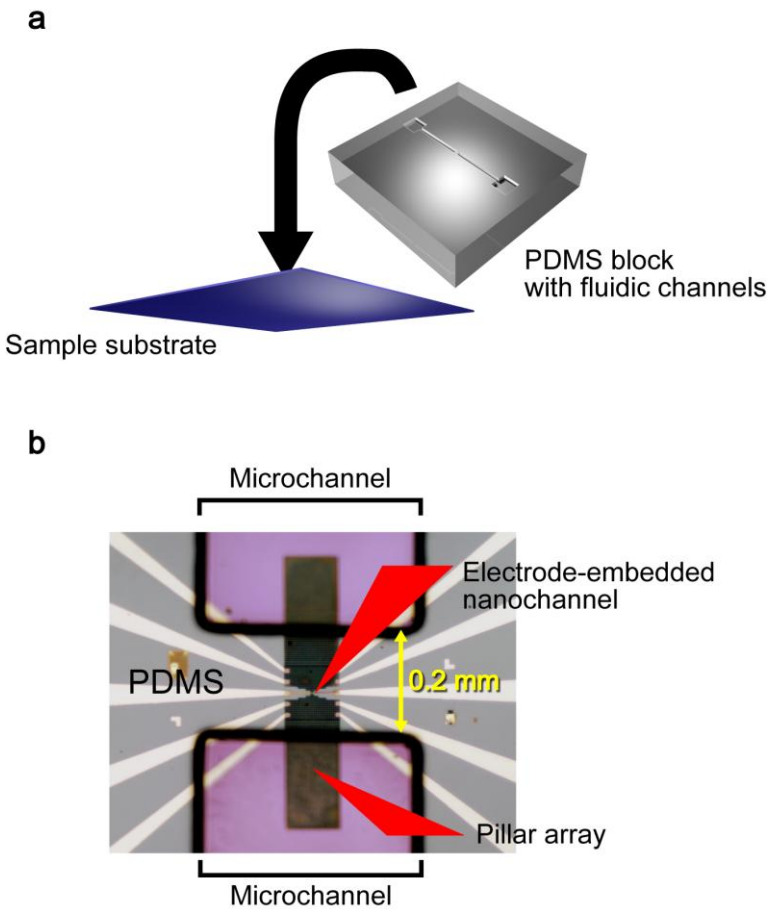

Supplementary Figure S3. Channel sealing with PDMS. **a,** A PDMS block with two channels formed on one side of the surface was prepared by curing it on an SU-8 mold. In prior to channel sealing, the sample substrate and the PDMS block was exposed to oxygen plasma for surface activation.[S1,S2] Subsequently, they are attached to each other. Permanent bonds are formed by these processes between the plasma-treated SiO_2 and PDMS. **b,** An optical microscopy image of sealed device. The purple colored regions are the PDMS channels. The 0.2 mm gap between the channels is used to seal the electrode-embedded nanochannel at the center. The micro-pillar arrays in the dark rectangular area served as spacer for preventing roof collapse.[S3]

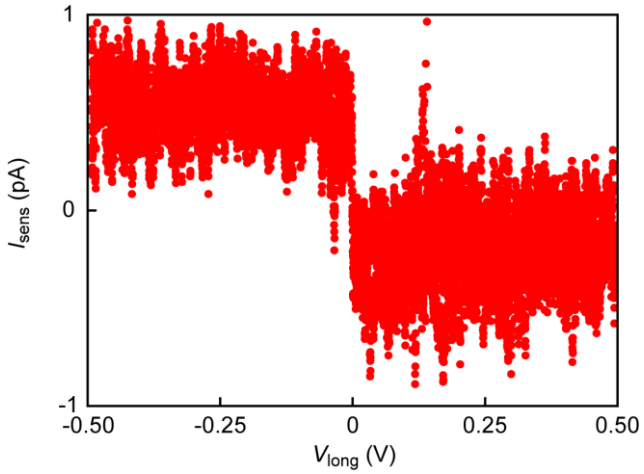

Supplementary Figure S4. Bias voltage dependence of transverse current in a 0.1 M KCl solution. The transverse current I_{sens} is smaller than 1 pA over the voltage range measured (-0.5 V $\leq$ V_{trans} $\leq$ 0.5V), below the resolution of a picoammeter used for the meausrement.

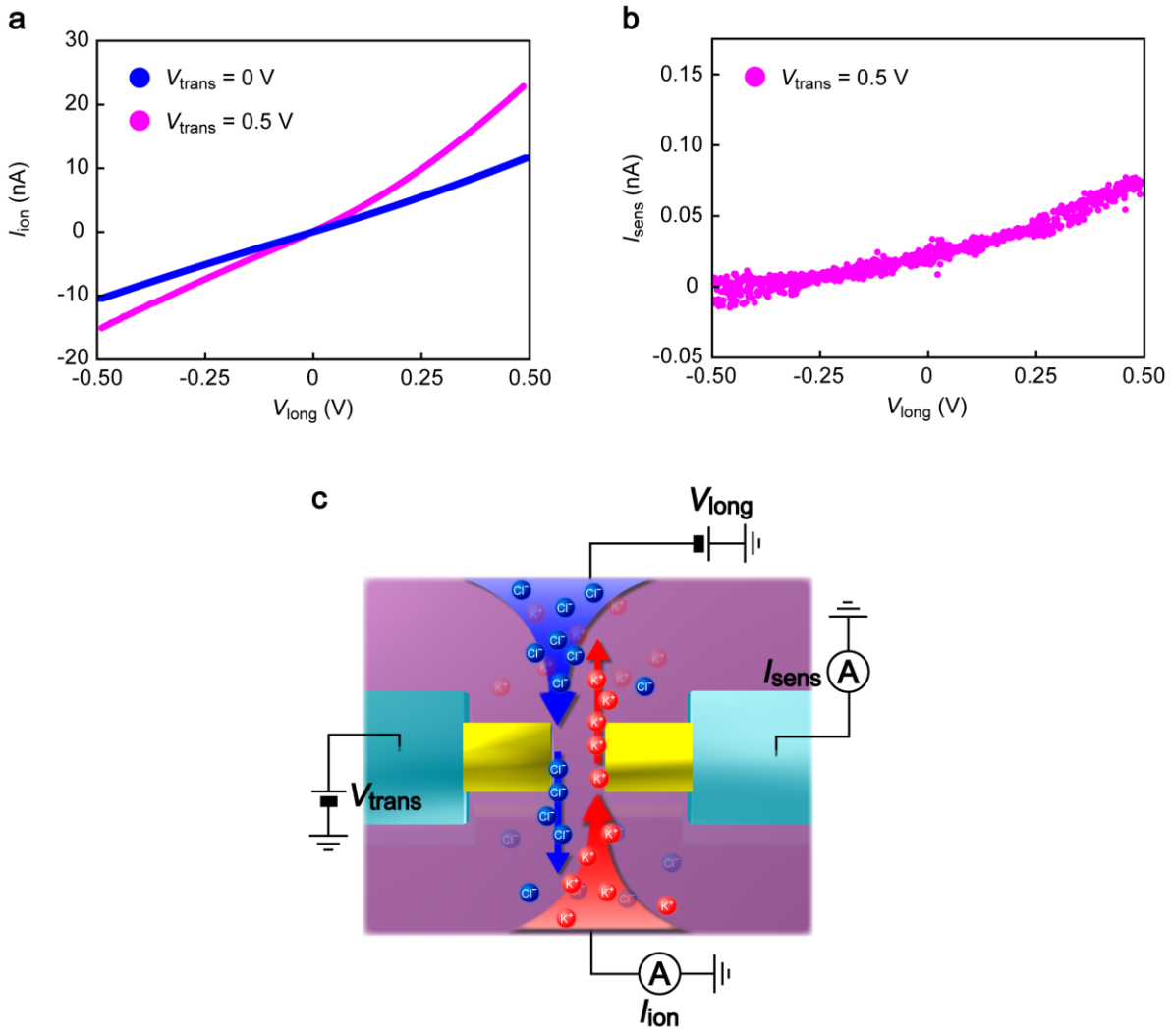

Supplementary Figure S5. Coupling between ionic current flowing through the trans-channel and the transverse electrodes. **a,** The trans-channel ionic current I_{ion} versus the longitudinal bias voltage characteristics in a 0.1 M KCl solution. V_{long} was swept at a rate of 5 mV/s from -0.5 V to 0.5 V. The transverse voltage V_{trans} of 0.5 V added to the transverse electrodes increased the longitudinal ionic conductance by approximately 30 % from 22.4 nS to 29.7 nS. **b,** Plots of the transverse current I_{sens} acquired simultaneously during the I_{ion}-V_{long} characteristics measurement. Addition of V_{long} enhanced I_{sens} from <1 pA to several tens of pA. Furthermore, we observed a small

change in I_{sens} with V_{long} suggesting a crosstalk between the two ion channels. **c,** Schematic describing the contribution of the transverse field induced antiparallel electroosmotic flows on the trans-channel and transverse ionic conductance. When the longitudinal field is absent, electric double layer forms on the polarizable Au electrodes that blocks I_{sens} to be < 1 pA. However, some parts of these ions are forced to move along the longitudinal direction when V_{long} is added and make contribution to I_{ion}. This not only makes the trans-channel conductance larger but also creates an ion pathway across the two transverse electrodes and enhances both the longitudinal and the transverse ionic conductance, as we have observed in (a) and (b).

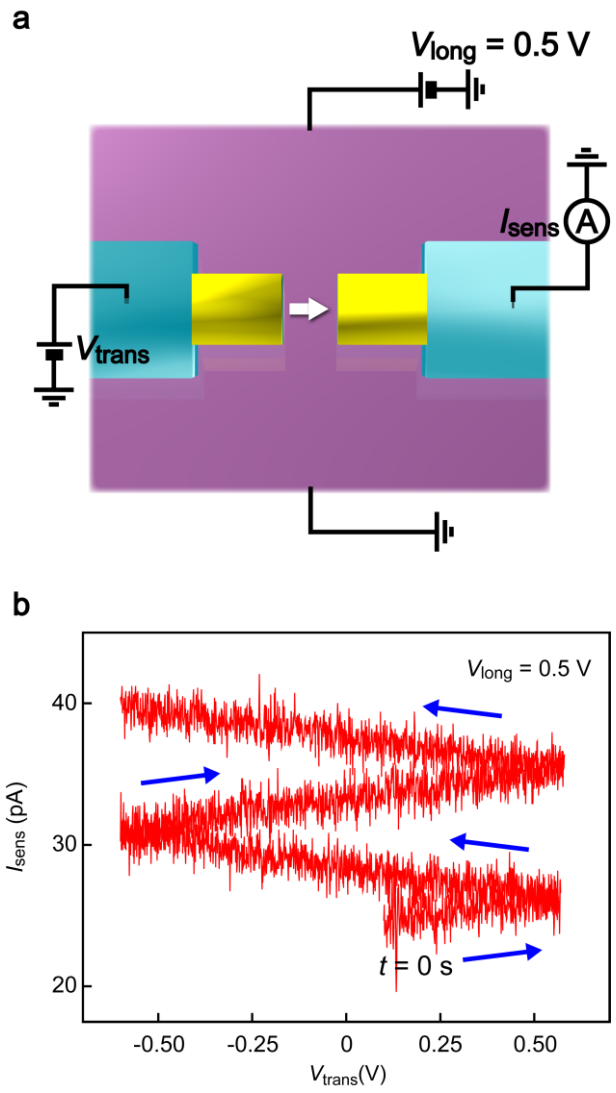

Supplementary Figure S6. V_{trans}-I_{sens} characteristics under longitudinal voltage of 0.5 V. **a.** A schematic illustration of the current measurement setup. The longitudinal voltage V_{long} was kept at 0.5 V while V_{trans} was swept from -0.5 V to 0.5 V and the current flowing through the two nanoelectrodes I_{sens} (white arrow) was recorded. **b,** The transverse current increases with time t regardless of V_{trans} until reaches a saturation at around 100 pA, suggesting Faradaic current contributions between the longitudinal Ag/AgCl electrode and the Au nanoelectrode. The blue arrows denote the direction of the bias sweep.

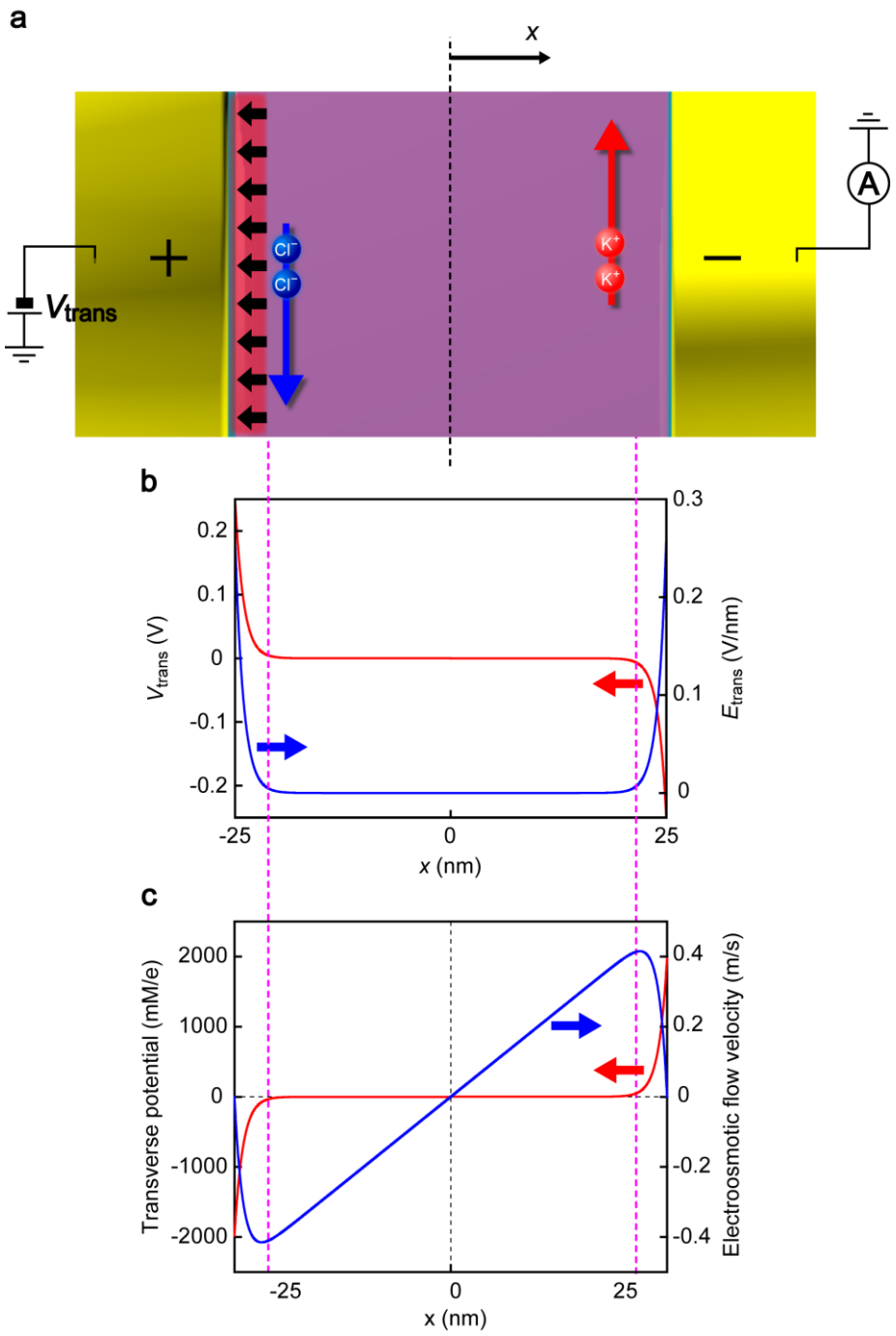

Supplementary Figure S7. Transverse electric field distribution and electroosmotic flow velocity in an electrode-embedded 50-nm channel filled with 0.1 M KCl. **a,** A schematic drawing depicting electroosmotic flow in the two-different directions at the positive and negative sides of the electrodes under a transverse voltage V_{trans}. The arrows

at the positively charged electrode indicate electrostatic field that tends to attract DNA molecules. **b,** Voltage drops (red) and corresponding electric field profile (blue) along the two transverse electrodes at V_{trans} = 0.5 V. The electric field decays exponentially with the distance from the electrode surface by screening. The dotted lines suggest the Debye length in a 0.1 M KCl solution. **c,** Transverse potential profile and electroosmotic flow velocity calculated following the previous work.[S4]

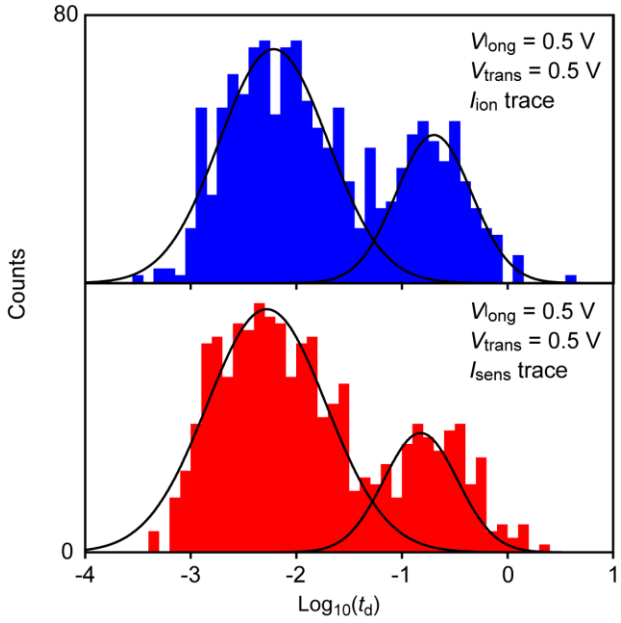

Supplementary Figure S8. Comparison of translocation duration distributions obtained for I_{ion} and I_{trans} transients. The trapping duration t_d corrected from the I_{ion} blockages detected at V_{long} = 0.5 V and V_{trans} = 0.5 V shows a bimodal distribution (blue). The simultaneously measured I_{sens} signals give very similar t_d distribution, thereby manifesting the synchronized I_{sens} variations to the I_{ion} blockades.

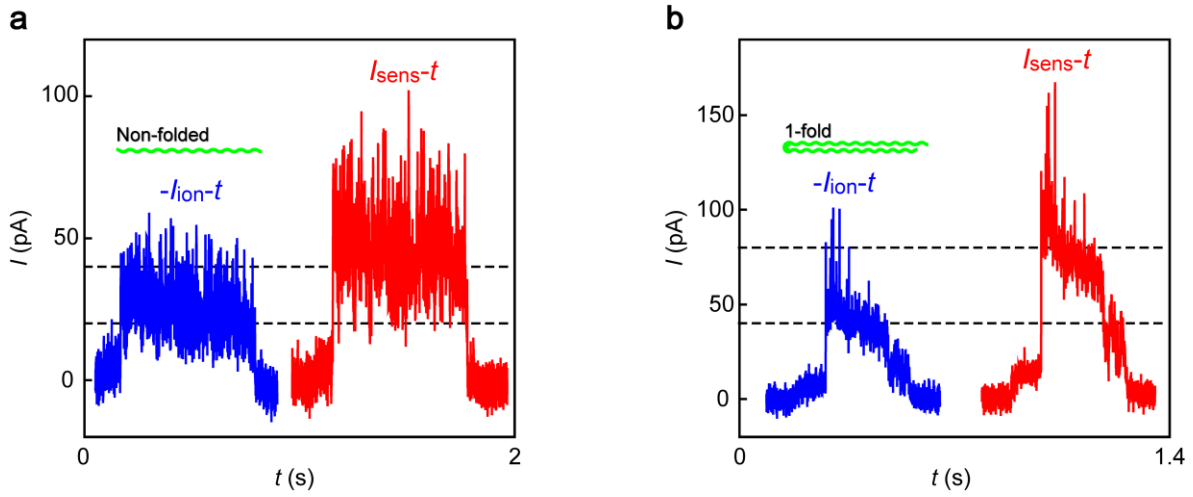

Supplementary Figure S9. I_{ion} **and** I_{sens} **traces obtained simultaneously at** V_{long} **0.5 V and** V_{trans} **= 0.5 V.** **a-b,** The I_{ion} blockage (blue) and corresponding I_{sens} signal (red) for (a) non-folded and (b) 1-folded states. The background has been offset to zero. The blockage curves are sign inverted. The broken lines are at 20 pA and 40 pA in (a) and 40 pA and 80 pA in (b).

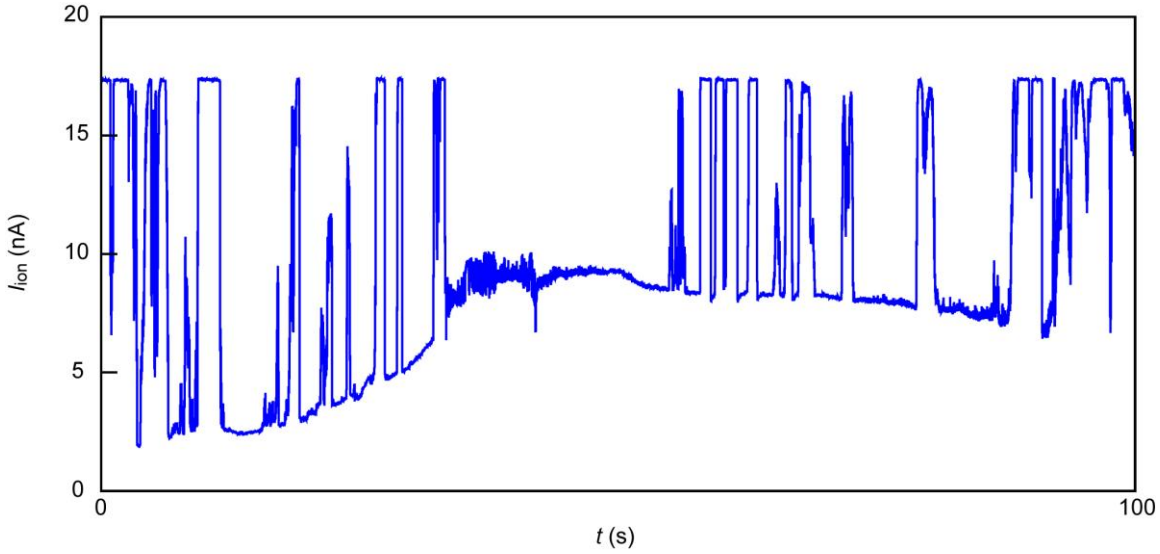

Supplementary Figure S10. I_{ion} **trace measured at** V_{long} **0.5 V and** V_{trans} **= 0.75 V.** The background current was about 17 nA. During the measurements, we observed large current drops by more than several nA as shown above. This anomalous feature is ascribable to blocking of the 50 nm channel by DNA molecules partially stapled at the positive electrode during translocation via the strong electrostatic binding.

4. Supplementary References

S1. Bhattacharya, S., Datta, A., Berg, J. M. & Gangopadhyay S. Studies on surface wettability of poly(dimethyl)siloxane(PDMS) and glass under oxygen-plasma treatment and correlation with bond strength. *J. Microelec. Sys.* **14**, 590-597 (2005).

S2. Berdichevsky, Y., Khandurina, J., Guttman, A., & Lo, Y. -H. UV/ozone modification of poly(dimethylsiloxane) microfluidic channels. *Sensors Actuators B: Chem.* **97**, 402-408 (2003).

S3. Tsutsui, M.; Sakon, R.; Iizumi, Y.; Okazaki, T.; Taniguchi, M. & Kawai, T. Single-molecule sensing electrode embedded in-plane nanopore. *Sci. Rep.* **1**, 46 (2011).

S4. Wong, C. T. A.; Muthukumar, M. Polymer capture by electro-osmotic flow of oppositely charged nanopore. *J. Chem. Phys.* **126**, 164903 (2007).